

Tyrosine Phosphatase STEP Is a Tonic Brake on Induction of Long-Term Potentiation

Kenneth A. Pelkey,^{1,2} Rand Askalan,² Surojit Paul,⁴
Lorraine V. Kalia,^{2,3} Tri-Hung Nguyen,⁴
Graham M. Pitcher,^{1,2} Michael W. Salter,^{1,2,3,5}
and Paul J. Lombroso⁴

¹Department of Physiology

²Programme in Brain and Behaviour
Hospital for Sick Children

³Institute of Medical Science
University of Toronto
Toronto Ontario, M5G 1X8
Canada

⁴The Child Study Center

Yale University School of Medicine
New Haven, Connecticut 06520

Summary

The functional roles of protein tyrosine phosphatases (PTPs) in the developed CNS have been enigmatic. Here we show that striatal enriched tyrosine phosphatase (STEP) is a component of the *N*-methyl-D-aspartate receptor (NMDAR) complex. Functionally, exogenous STEP depressed NMDAR single-channel activity in excised membrane patches. STEP also depressed NMDAR-mediated synaptic currents whereas inhibiting endogenous STEP enhanced these currents. In hippocampal slices, administering STEP into CA1 neurons did not affect basal glutamatergic transmission evoked by Schaffer collateral stimulation but prevented tetanus-induced long-term potentiation (LTP). Conversely, inhibiting STEP in CA1 neurons enhanced transmission and occluded LTP induction through an NMDAR-, Src-, and Ca²⁺-dependent mechanism. Thus, STEP acts as a tonic brake on synaptic transmission by opposing Src-dependent upregulation of NMDARs.

Introduction

Fast excitatory synaptic transmission within the mammalian central nervous system (CNS) is principally mediated by the transmitter glutamate acting at postsynaptic AMPA and NMDA subtypes of ionotropic glutamate receptors (Edmonds et al., 1995; Hollmann and Heinemann, 1994). Activation of the NMDA subtype of glutamate receptor is crucial for development, neuroplasticity, and excitotoxicity in the CNS (Dingledine et al., 1999; McBain and Mayer, 1994). The function of NMDA receptors (NMDARs) is dynamically tuned to the state of the neuron by intracellular biochemical processes, including tyrosine phosphorylation/dephosphorylation (Wang and Salter, 1994). NMDAR function is upregulated by the nonreceptor tyrosine kinase Src (Yu et al., 1997), which serves as a point of convergence through which signaling cascades modulate NMDAR function (Huang et al., 2001; Lu et al., 1999) and is required for NMDAR-dependent long-term potentiation (LTP) in the hippocampus

(Huang et al., 2001; Lu et al., 1998). Thus, tyrosine phosphorylation has emerged as a key regulator of NMDAR function and thereby of excitatory synaptic transmission.

The level of tyrosine phosphorylation of NMDARs is, however, not determined by Src alone but by the balance between its activity and that of a phosphotyrosine phosphatase (PTP). The endogenous PTP regulating the function of NMDARs is known to be intimately associated with the receptor (Wang et al., 1996) but the identity of this PTP has remained elusive. PTPs are a large, structurally diverse superfamily of enzymes which may have exquisite specificity of their effects in cells (Tonks and Neel, 2001). A number of PTPs have been shown to be expressed in the CNS, the majority of which are receptor-type PTPs, which have been implicated in neuronal morphogenesis, neural development, and axon guidance (Arregui et al., 2000; Naegele and Lombroso, 1994; Stoker and Dutta, 1998; Stoker, 2001). The level of expression of such PTPs typically is dramatically downregulated during ontogeny, making these unlikely candidates for the PTP regulating NMDARs, which is expressed in adult neurons. One family of PTPs whose expression level is high in the adult is the striatal enriched phosphatase (STEP) family. STEPs are brain-specific, nonreceptor-type PTPs that were originally identified as highly enriched within neurons of the striatum (Lombroso et al., 1991, 1993), although more extensive mapping studies found them in multiple brain regions including the hippocampus and cerebral cortex (Boulanger et al., 1995). STEP immunoreactivity has been observed in postsynaptic densities (Oyama et al., 1995), raising the possibility that this PTP might postsynaptically modulate glutamatergic transmission. In the present study, we investigated whether STEP regulates NMDAR function in opposition to Src at excitatory synapses.

Results

STEP Is a Component of the NMDAR Complex

Studies on spinal cord neurons first demonstrated that the PTP opposing Src is intimately associated with the NMDAR complex (Wang et al., 1996). We therefore used homogenates from the spinal cord to determine if STEP associates with NMDARs. We found that STEP₆₁, the highest molecular weight isoform of the STEP family (Boulanger et al., 1995), was expressed in the spinal cord (Figure 1A). In order to determine whether STEP and NMDA channels are associated physically, we immunoprecipitated membrane proteins with monoclonal antibodies specifically directed against STEP (anti-STEP; Boulanger et al., 1995) or NR1, a requisite subunit of NMDARs (Dingledine et al., 1999). We used non-denaturing conditions to solubilize membrane proteins from spinal cord homogenates and found that immunoprecipitating with anti-STEP led to co-precipitation of NR1 (Figure 1A). Conversely, immunoprecipitation with anti-

⁵Correspondence: mike.salter@utoronto.ca

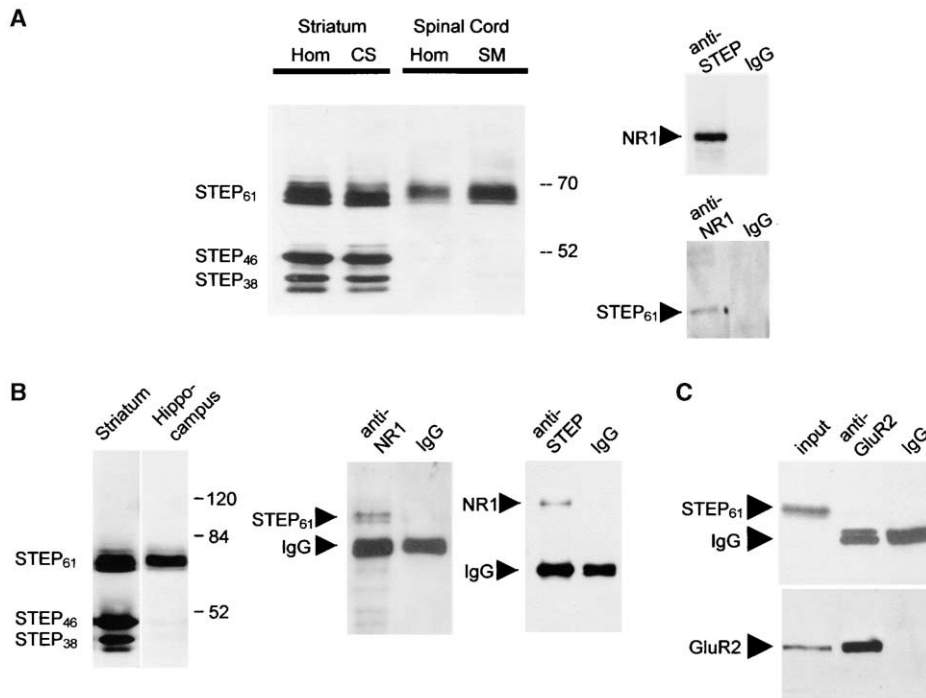


Figure 1. STEP Associates with NMDARs

(A) In the left panel, immunoblot analysis of spinal cord homogenates (Hom) and solubilized membranes (SM) with anti-STEP antibody revealed a protein band of approximately 61 kDa. Striatal homogenates (Hom) and crude synaptosomes (CS) probed as positive controls contained the same immunopositive band as well as other lower molecular weight STEP isoforms. The right panels depict representative immunoprecipitation experiments from spinal cord membranes with anti-STEP (upper panel), anti-NR1 (lower panel), or nonspecific IgG (both panels) under nondenaturing conditions. Proteins were resolved by SDS-PAGE, transferred to nitrocellulose, and analyzed by sequential immunoblotting with anti-NR1 (upper panel), or anti-STEP (lower panel).

(B) The left panel shows an immunoblot analysis of striatal and hippocampal homogenates (Hom) probed with anti-STEP. The middle panel shows an immunoblot probed with anti-STEP of proteins coimmunoprecipitating with anti-NR1 from hippocampal homogenates (left lane, anti-NR1). In the right lane, the anti-NR1 antibody was run to show the position of the IgG heavy chain (IgG). The right panel displays an immunoblot probed with anti-NR1 antibody of proteins co-precipitating with anti-STEP from hippocampal homogenates (left lane, anti-STEP). In the right lane, the immunoprecipitation was performed using nonspecific IgG. In both (A) and (B), co-precipitation of STEP by anti-NR1 and of NR1 by anti-STEP was prevented when denaturing solubilization conditions were used, whereas the immunoprecipitation of NR1 or STEP by the corresponding antibodies was not affected (data not shown).

(C) shows a representative immunoblot probed with anti-STEP antibody (upper panel) of proteins coimmunoprecipitating with anti-GluR2 or nonspecific IgG from hippocampal homogenates (middle and right lanes, respectively). The blot was stripped and reprobed with anti-GluR2 (lower panel). The starting homogenate was run in the left lane (Input).

NR1 co-precipitated STEP₆₁ (Figure 1A). Neither NR1 nor STEP₆₁ was precipitated by nonspecific IgG. Because NMDARs in hippocampal neurons are also regulated by tyrosine phosphorylation, we examined STEP expression and association with NMDARs in the hippocampus. As with the spinal cord, we found that the major STEP isoform expressed in the hippocampus is STEP₆₁ (Figure 1B). Immunoprecipitating with anti-NR1 led to co-precipitation of STEP₆₁ from hippocampal homogenates, and immunoprecipitation with anti-STEP co-precipitated NR1 (Figure 1B). From these data together, we concluded that STEP₆₁ and NMDAR subunit proteins associate, directly or indirectly, *in vitro*. Therefore, STEP₆₁ may be a component of the NMDAR complex *in situ* and thus may be strategically positioned to regulate NMDAR function. In contrast, STEP did not co-precipitate with the AMPA receptor subunit GluR2 (Figure 1C), indicating that STEP may interact selectively with NMDARs but not with AMPARs.

Administering STEP Reduces NMDA Single-Channel Activity and NMDAR-Mediated Synaptic Currents

Inhibiting Src, thereby allowing the unopposed action of the endogenous PTP, depresses NMDA channel gating by decreasing mean channel open time (t_o) and open probability (P_o), and causes characteristic changes in channel kinetics (Yu et al., 1997). To determine whether STEP downregulates NMDA channel gating, we recorded NMDAR-mediated single-channel currents using inside-out patches excised from spinal cord neurons. We found that applying purified, recombinant STEP to the cytoplasmic face of the patches depressed channel activity without altering single-channel conductance (Figure 2A). On average, P_o decreased to $46\% \pm 7.4\%$ of that during the control period just prior to applying STEP and there was a reduction in t_o to $71\% \pm 7.3\%$ of control (mean \pm SEM; $n = 5$ patches). STEP also caused marked changes in the distributions of open

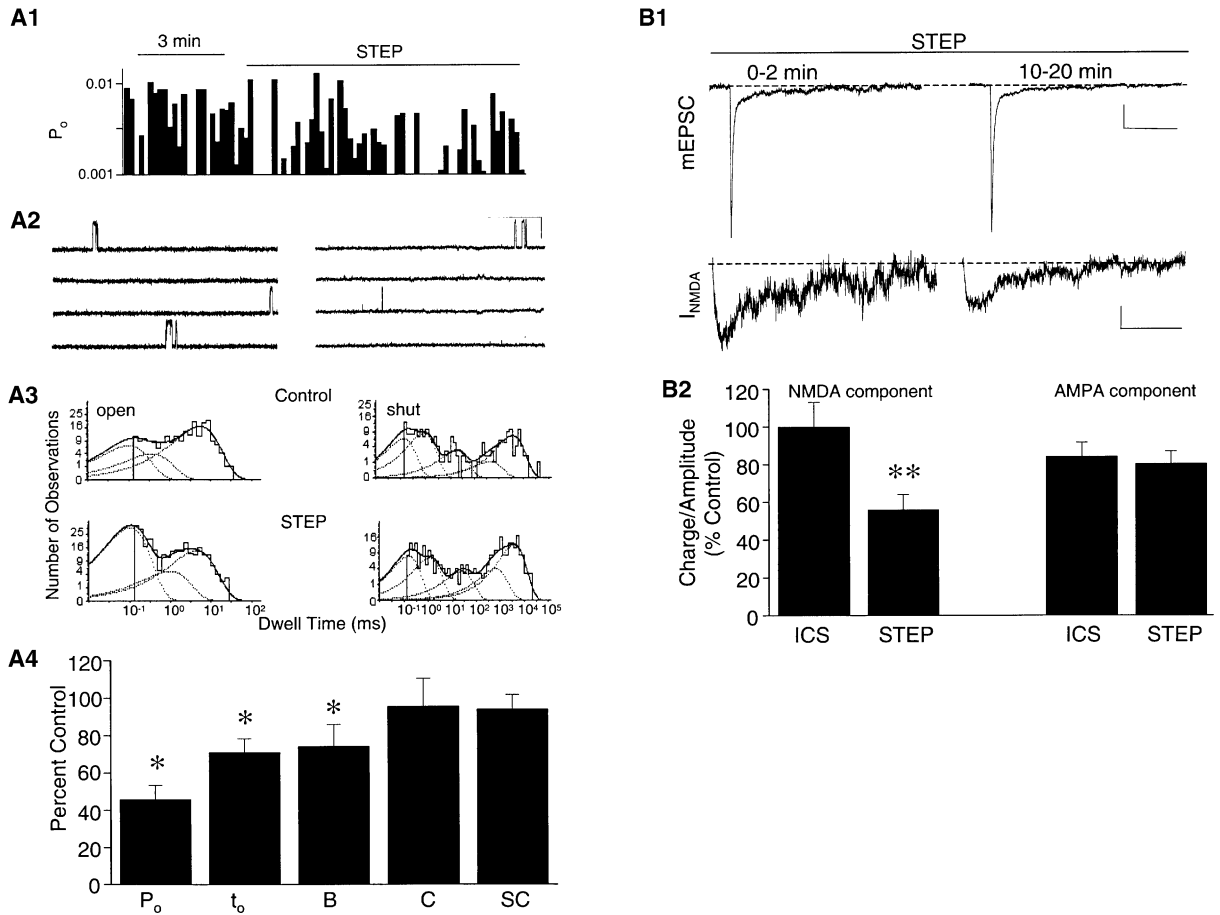


Figure 2. Recombinant STEP Depresses NMDAR Activity

(A1) A continuous record of NMDA channel open probability (P_o) before and during application of recombinant STEP to the cytoplasmic face of a membrane patch is shown. P_o was calculated in bins of 10s in duration.

(A2) Continuous sample traces of currents from the same patch used in (A1) obtained before (left set of traces) and during STEP (5 μ g/ml; right set of traces) application are shown (calibration bars are 100 ms/3 pA).

(A3) Dwell-time histograms of open and shut times before (upper panels) and during (lower panels) STEP application are shown. Dashed lines indicate the individual exponential components of the open and shut times and solid lines show the sum of the components. The average time constants of the individual exponential components before STEP application were (mean \pm SEM) 0.10 ± 0.02 , 1.3 ± 0.24 , and 5.6 ± 0.24 ms (open times) and 0.14 ± 0.03 , 0.8 ± 0.07 , 13.0 ± 1.9 , 226 ± 119 , and 1449 ± 876 ms (closed times); these time constants were not significantly altered by STEP application.

(A4) A bar graph summarizing the effects of STEP on single channel parameters is shown ($n = 5$ patches). Values are the means \pm SEM. P_o , open probability; t_o , mean open time; B, burst duration; C, cluster duration; SC, supercluster duration. (* $p < 0.05$, paired t test before versus during STEP.)

(B1) Traces of representative averaged mEPSCs (top traces) or NMDA components (I_{NMDA}) (lower traces) obtained from 0–2 min or from 10–20 min after breakthrough with recombinant STEP in the recording pipette are shown. We constructed I_{NMDA} by subtracting, from the averaged mEPSC, a current decaying at a single exponential rate equal to the fast component. Scale bars for mEPSCs are 50 ms/5 pA and for I_{NMDA} are 50 ms/1 pA.

(B2) The mean changes in the NMDA and AMPA components of averaged mEPSCs recorded at 10–20 min after breakthrough are expressed as a percentage of control mEPSCs obtained 0–2 min after breakthrough during recordings with regular intracellular solution (ICS; $n = 8$ cells) or ICS supplemented with recombinant STEP ($n = 6$ cells). Peak mEPSC amplitude was measured to determine the AMPA component of averaged mEPSCs and integrated current during I_{NMDA} (charge) was measured to determine the NMDA component of averaged mEPSCs. (** $p < 0.01$; t test versus ICS.)

and shut times, changes which were due to alterations in the relative weighting of the components rather than to significant changes in the values of the time constant for each component. STEP caused an increase in the area of the shortest open time and longest shut time with concomitant decreases in the area of the longest open times and shortest closed times (Figure 2A3). STEP also produced a decrease in the duration of bursts (Fig-

ure 2A4) and in the total open time and number of openings during the bursts (not illustrated). Thus, the effects of STEP were similar to those predicted for the endogenous PTP.

Because the kinetic properties of NMDA channels shape synaptic NMDAR-mediated responses (Edmonds et al., 1995), we predicted that STEP would depress NMDAR synaptic currents. We therefore studied the ef-

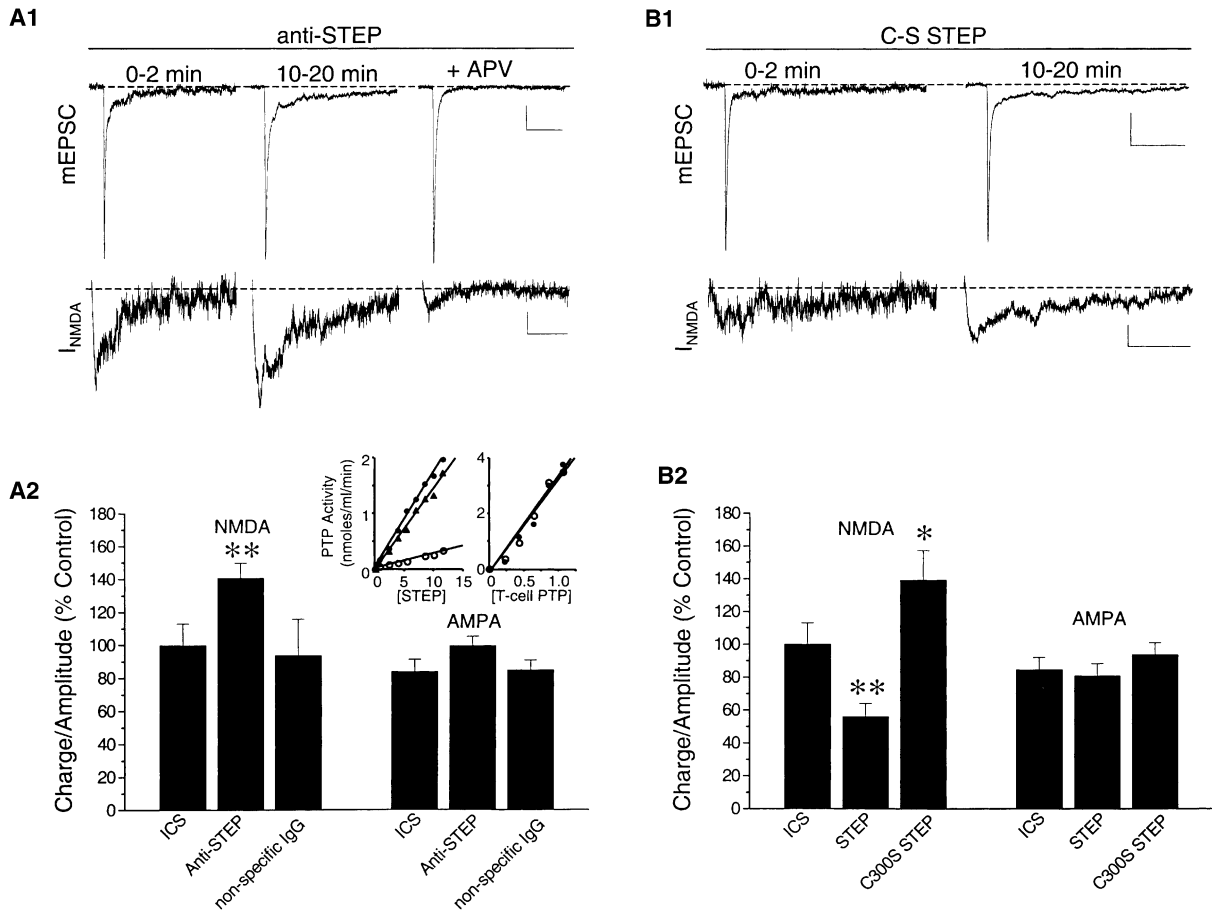


Figure 3. Synaptic NMDARs Are Tonicly Inhibited by Endogenous STEP

(A1–B1) Representative averaged mEPSCs (top traces) or NMDA components (I_{NMDA}) (lower traces) obtained from 0–2 min after breakthrough with anti-STEP (A1) or c300S STEP (B1) in the recording pipette are displayed. In (A1), APV (50 μ M) was added to the bathing solution at the end of the experiment to demonstrate that the late component of the mEPSC is mediated by NMDAR activation. Scale bars for mEPSCs are 50 ms/5 pA and for I_{NMDA} are 50 ms/1 pA. (A2–B2) Mean changes in the NMDA and AMPA components of averaged mEPSCs recorded at 10–20 min after breakthrough are expressed as a percentage of control mEPSCs obtained 0–2 min after breakthrough during recordings with ICS ($n = 8$ cells) or ICS supplemented with anti-STEP (A2; $n = 7$ cells), nonspecific IgG (A2; $n = 5$ cells), or C300S STEP (B2; $n = 6$ cells) (** $p < 0.01$, * $p < 0.05$; t test versus ICS; for anti-STEP versus IgG in (A2), $p < 0.05$). The inset in (A2) shows a representative phosphatase activity assay for recombinant STEP (left panel) and T cell phosphatase (right panel) in the absence (\bullet both panels) and presence (\circ both panels) of anti-STEP or nonspecific IgG (\blacktriangle left panel only). The concentrations of STEP and T cell PTP are in pmol. In (B2), the effect of STEP is replotted for comparison with C300S STEP.

ffects of STEP on miniature excitatory postsynaptic currents (mEPSCs) during whole-cell recordings from cultured dorsal horn neurons (Figure 2B). Administering recombinant STEP intracellularly through the recording pipette led to a decline in the NMDAR-mediated component of the mEPSCs: on average the NMDAR-mediated component of mEPSCs recorded 10–20 min after the start of recording was reduced to $56\% \pm 8\%$ of the initial value during the first 2 min of recording ($n = 7$ cells). In contrast to the effect of STEP on the NMDAR component of mEPSCs, STEP produced no effect on the AMPAR-mediated component. Thus, STEP selectively depressed NMDARs, but not AMPARs, at synapses.

Endogenous STEP Tonicly Depresses NMDAR Function in Opposition to Src

The effects of STEP on NMDAR single-channel kinetics and NMDAR mEPSCs were similar to those caused by

inhibiting Src (Yu et al., 1997), indicating that depression of NMDAR function by STEP resembles that induced by the endogenous PTP. To test whether this endogenous PTP is STEP, we intracellularly applied the anti-STEP antibody (Boulanger et al., 1995). In PTP activity assays, we found that this antibody inhibited the function of recombinant STEP but did not affect the activity of purified T cell phosphatase catalytic domain (inset Figure 3A) or of recombinant PTP-1B (see Experimental Procedures). Thus, the anti-STEP antibody inhibits STEP function but is not a general PTP inhibitor. The anti-STEP antibody was found to increase the NMDAR-mediated component of mEPSCs to $141\% \pm 9\%$ of the initial level in dorsal horn neurons ($n = 7$ cells; Figure 3A). On the other hand, a nonspecific IgG antibody did not significantly alter the NMDAR component of the mEPSCs ($n = 6$ cells). Neither the anti-STEP antibody nor nonspecific IgG affected the AMPAR-mediated component of the

mEPSCs. As an independent test to determine the effect of inhibiting endogenous STEP, we intracellularly administered a dominant-negative mutant STEP (C300S STEP) (Lombroso et al., 1993) (Figure 3B). Including C300S STEP in the recording pipette led to an increase in the NMDAR-component of mEPSCs; the AMPAR-component of the mEPSCs was unaffected by C300S STEP (Figure 3B).

In CA1 pyramidal neurons recorded from acute hippocampal slices, we found that intracellularly administered anti-STEP increased the amplitude of pharmacologically isolated NMDAR EPSCs evoked by Schaffer collateral stimulation (Figure 4A): 20 min into recordings, NMDAR-mediated EPSCs were $184\% \pm 31\%$ ($n = 5$) of the initial level when anti-STEP was intracellularly administered as compared with $106\% \pm 12\%$ ($n = 6$) in controls without anti-STEP ($p < 0.05$) or $92\% \pm 15\%$ ($n = 5$) with administration of nonspecific IgG ($p < 0.05$). Importantly, the current-voltage relationship of the NMDAR EPSCs after potentiation by anti-STEP was not different from that of control or IgG recordings (Figure 4B) and therefore, the upregulation of NMDAR function by inhibiting STEP does not alter depression of NMDARs by extracellular Mg^{2+} . Taken together these results indicate that in dorsal horn and CA1 neurons there is ongoing suppression of the function of synaptic NMDARs by endogenous STEP.

If the ongoing depression of NMDARs by STEP directly opposes Src then blocking this kinase is predicted to occlude the effect of exogenously administering STEP. We tested this prediction using dorsal horn neurons which were pre-treated with the Src kinase inhibitor PP2 (Hanke et al., 1996) in order to depress NMDAR currents prior to recording (Figure 5). STEP, administered intracellularly in the continued presence of PP2, did not further depress the NMDAR-mediated component of mEPSCs (Figures 5A and 5C). Conversely, in the presence of PP3, an inactive analog of PP2, intracellular application of STEP depressed the NMDAR-component of the mEPSCs (Figures 5B and 5C), and the extent of the depression was not different from that produced by STEP alone (cf. Figure 2B). If Src and STEP act reciprocally, it is further predicted that inhibiting Src will prevent the upregulation of NMDARs caused by anti-STEP. Consistent with this prediction, we found that applying PP2 prevented the increase in the NMDAR-component of the mEPSCs by anti-STEP; PP3 did not affect the anti-STEP-induced increase in NMDAR mEPSCs (Figure 5C). Thus, the effects of applying exogenous STEP or of inhibiting endogenous STEP are prevented by blocking Src. These findings indicate that STEP opposes the effect of Src on NMDARs. Since the STEP isoform which is part of the NMDAR complex is STEP₆₁, we conclude that STEP₆₁ is the PTP that opposes Src in the regulation of NMDARs.

Administering STEP Prevents Tetanus-Induced LTP

Activation of Src in the CA1 region of the hippocampus is produced by tetanic stimulation of Schaffer collateral inputs and is required postsynaptically for induction of long-term potentiation (LTP) at Schaffer collateral-CA1 synapses (Lu et al., 1998). Because STEP opposes the

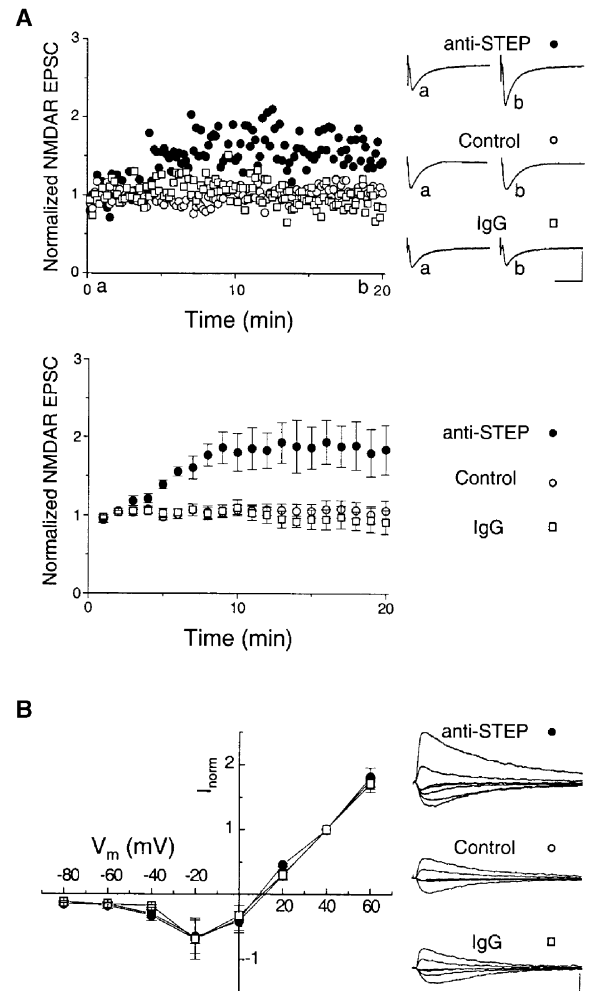


Figure 4. STEP Inhibition Potentiates NMDAR-Mediated EPSCs in Hippocampal Neurons without Altering Voltage-Dependent Mg^{2+} Inhibition

(A) The upper panel displays scatter plots of the normalized NMDA EPSC peak amplitude for representative cells recorded with control ICS (\circ), or with ICS supplemented with anti-STEP ICS (\bullet) or with nonspecific IgG (\square). The traces at right are the average of six consecutive EPSCs obtained at the times indicated (Scale bars are 50 ms/50 pA). The lower panel is a plot of the average NMDAR EPSC amplitude versus time for experiments performed with anti-STEP supplemented ICS (\bullet , $n = 5$), control ICS (\circ , $n = 6$), or nonspecific IgG supplemented ICS (\square , $n = 5$).

(B) The current-voltage (I-V) relationships for pharmacologically isolated NMDAR EPSCs during intracellular administration of anti-STEP (\bullet , $n = 5$), control solution (\circ , $n = 5$), or nonspecific IgG (\square , $n = 4$) are plotted. I-V relationships for individual cells were obtained at the end of the recording period 20 min after breakthrough, and the peak amplitude of the EPSCs obtained at holding potentials from -80 to $+60$ were normalized to that at $+40$ mV. On the right superimposed NMDAR EPSC traces at membrane potentials from -80 to $+40$ mV are shown in steps of 20 mV for three representative cells (scale bars are 100 ms/200 pA).

effect of Src on NMDAR function, associates with hippocampal NMDARs, and regulates NMDARs at Schaffer collateral-CA1 synapses, we questioned whether STEP may participate in synaptic plasticity in CA1 neurons. We used whole-cell recordings from CA1 neurons in

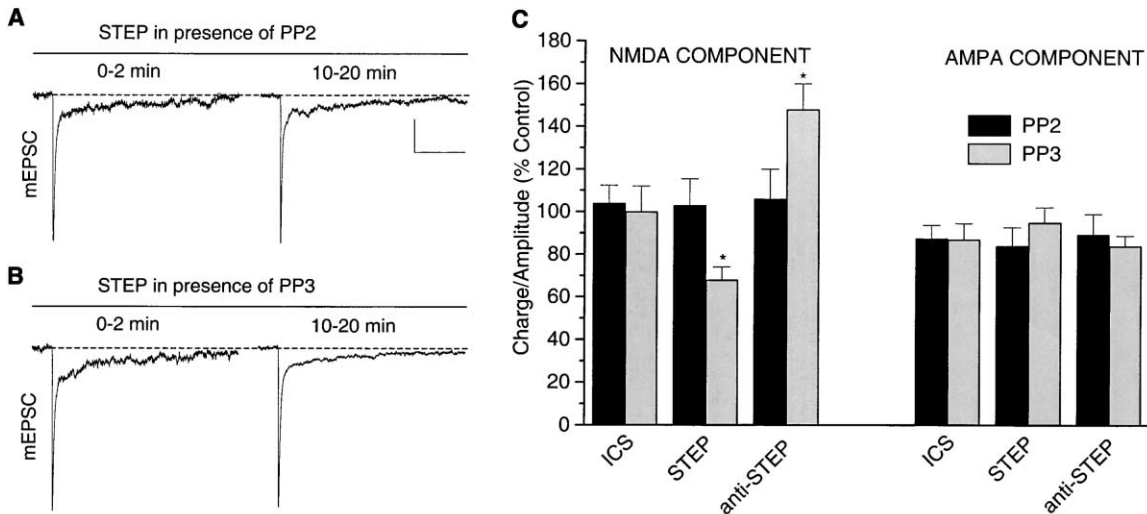


Figure 5. Regulation of NMDAR Currents by STEP Requires Endogenous Src Kinase Activity

(A) Traces are representative averaged mEPSCs obtained from 0–2 min after breakthrough or 10–20 min after breakthrough with STEP in the recording pipette in the presence of PP2 (upper panel) or PP3 (lower panel) containing extracellular solution. Scale bars are for both sets of traces and are 50 ms/5 pA.

(B) Mean changes in the NMDA and AMPA component of mEPSCs in the presence of PP2 (black bars) or PP3 (gray bars) with ICS ($n = 6$ for PP2 and 5 for PP3), STEP ($n = 4$ for PP2 and 4 for PP3), or anti-STEP ($n = 6$ for PP2 and 5 for PP3) in the recording pipette are depicted. (* $p < 0.05$, t test versus ICS.)

acute hippocampal slices to administer STEP postsynaptically and simultaneously recorded field potentials. STEP was found to have no effect on baseline excitatory postsynaptic potentials (EPSPs) at these synapses ($n = 6$ cells; Figure 6). Tetanic stimulation of the Schaffer collateral inputs produced post-tetanic potentiation in neurons in which exogenous STEP was applied, but over the subsequent 30 min, the EPSPs returned to the level prior to tetanus: EPSP slope was $103\% \pm 11\%$ ($p > 0.5$) of the pre-tetanus level 30 min after tetanus. On the other hand, in the field recordings from these slices and also in control whole-cell recordings without exogenous STEP ($n = 8$), tetanic stimulation produced post-tetanic potentiation and also a lasting increase in EPSPs which persisted throughout the recording period (Figure 6). Thus, administering STEP into CA1 neurons prevented the induction of LTP by tetanic stimulation of Schaffer collaterals.

Inhibiting Endogenous STEP Enhances EPSPs and Occludes Tetanus-Induced LTP

We next investigated the role of endogenous STEP in synaptic transmission and plasticity in CA1 neurons by administering anti-STEP intracellularly during whole-cell recordings (Figure 7). Anti-STEP produced a progressive increase in EPSPs over the first 20 min of recording reaching a level of $181\% \pm 18\%$ of the initial level ($p < 0.01$; $n = 9$ cells). Subsequent tetanic stimulation of the Schaffer collateral input caused a transient post-tetanic potentiation of the EPSPs but no lasting increase as compared with the period just prior to tetanus: 30 min after tetanus EPSP slope was on average $100\% \pm 14\%$ ($p > 0.5$) of the level just prior to tetanus, whereas fEPSP slope increased to $138\% \pm 7\%$ ($p < 0.01$). Similarly, introduction of C300S STEP into CA1 neurons through

the recording electrode resulted in a progressive increase in EPSPs to $189\% \pm 14\%$ of the initial level 20 min into the recording ($p < 0.05$; $n = 4$ cells; Figure 8B). Conversely, in cells recorded with control intracellular solution lacking anti-STEP or C300S STEP (Figures 6B, 7B, and 8B), baseline EPSPs did not change during the pre-tetanus period of recording and Schaffer collateral tetanus induced a persistent increase in EPSPs ($176\% \pm 22\%$; $p < 0.01$). Thus, inhibiting STEP caused a sustained potentiation of EPSPs which occluded induction of LTP.

Enhancement of EPSPs by Inhibiting STEP Is NMDAR, Src, and Ca^{2+} Dependent

The EPSPs in CA1 neurons are primarily mediated by AMPARs, which are not directly regulated by tyrosine phosphorylation/dephosphorylation (Huang et al., 2001; Lu et al., 1998; O'Dell et al., 1991). We therefore predicted that the upregulation of CA1 EPSPs observed during intracellular administration of anti-STEP would require NMDAR activity. During NMDAR blockade, with bath application of the noncompetitive NMDAR antagonist MK801, we found that administering anti-STEP intracellularly caused no change in EPSP slope: EPSP slope was $105\% \pm 6.6\%$ ($p > 0.5$; $n = 4$ cells) of the initial level after 20 min of whole-cell recording (Figures 8A and 8B). Furthermore, the increase in EPSP slope produced by anti-STEP was prevented when a peptide, Src40-58, which prevents Src-induced enhancement of NMDARs (Yu et al., 1997), was co-administered with anti-STEP through the recording electrode (Figures 8A and 8B). Lastly, we determined whether the enhancement of AMPAR EPSPs caused by inhibiting STEP depended upon raising intracellular Ca^{2+} . We found that when the buffering capacity of the intracellular environ-

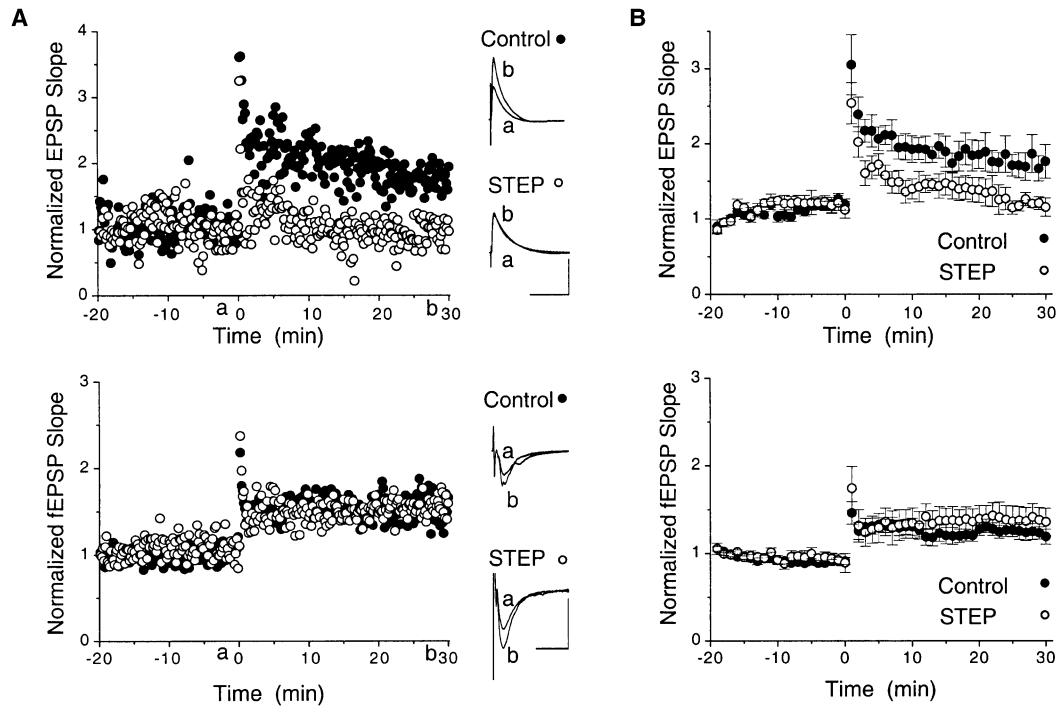


Figure 6. Administering STEP Postsynaptically Prevents Induction of LTP at Schaffer Collateral CA1 Synapses

(A) Scatter plots of EPSP slope (upper graph) and simultaneously recorded fEPSP slope (lower graph) from individual representative experiments with (○) or without (●) STEP in the whole-cell recording solution are shown. EPSP and fEPSP slopes were normalized to the average level during the first 5 min of recording. Tetanus was delivered at time 0 min in this and all subsequent graphs. Each trace to the right of the plots is the average of six consecutive EPSPs or fEPSPs recorded at the times indicated. Scale bars for this and all subsequent traces are 10 mV/200 ms for EPSPs and 1 mV/20 ms for fEPSPs.

(B) The top graph is a plot of average EPSP slope versus time for experiments with (○, $n = 6$) or without (●, $n = 8$) active STEP included in the whole-cell recording solution. The bottom graph shows the averaged slope of field EPSPs (fEPSPs) measured during experiments when whole-cell recordings were done with (○) and without STEP (●).

ment was increased by including 10 mM BAPTA in the intracellular recording solution, administering anti-STEP had no effect on AMPAR EPSPs (Figure 8B). Thus, the lasting potentiation of EPSPs produced by inhibiting STEP does not occur through a direct effect on AMPA receptors, but rather is dependent upon NMDAR activation, Src-mediated upregulation of NMDAR function, and a rise in intracellular Ca^{2+} . From these results together, we conclude that STEP functions as a tonic brake on synaptic transmission at Schaffer collateral-CA1 synapses by opposing Src-mediated enhancement of NMDARs, thus governing the induction of long-term plastic changes in synaptic efficacy.

Discussion

The main goal achieved in the present work is the identification of an endogenous PTP that counterbalances the tyrosine kinase Src to regulate the function of NMDARs. The principal requirements for such an endogenous PTP, as inferred from previous studies (Wang et al., 1996; Wang and Salter, 1994; Yu et al., 1997), are that it must be intimately associated with the NMDAR complex and must decrease the activity of NMDARs by opposing Src-mediated upregulation. Here, we find that applying purified STEP depresses NMDAR currents in excised patches and at synapses. Conversely, we find

that inhibiting endogenous STEP, either with a function-blocking antibody or a dominant-inhibitory STEP mutant protein, increases NMDAR currents as expected for the effects of inhibiting the endogenous PTP (Wang et al., 1996; Wang and Salter, 1994). Both the depression of NMDAR currents produced by STEP and the enhancement of NMDAR currents by inhibiting STEP require the activity of Src. Because we find that it is the 61 kDa isoform of STEP that coimmunoprecipitates with NMDAR subunits, we conclude that STEP₆₁ is an endogenous PTP that regulates the function of NMDARs in opposition to Src.

A second main conclusion from our work is that ongoing STEP-mediated depression of NMDAR activity tonically regulates synaptic efficacy in CA1 hippocampal neurons: administering active recombinant STEP directly into CA1 neurons prevents the induction of LTP by tetanic stimulation and, conversely, inhibiting endogenous STEP in these neurons enhances synaptic transmission and occludes tetanus-induced LTP. Recent models of NMDAR-dependent LTP postulate that the ultimate mechanism through which this form of plasticity is expressed involves postsynaptic enhancement of the channel activity and/or cell-surface expression of AMPARs (Malenka and Nicoll, 1999; Malinow et al., 2000; Soderling and Derkach, 2000). However, because these receptors are not directly regulated by tyrosine phos-

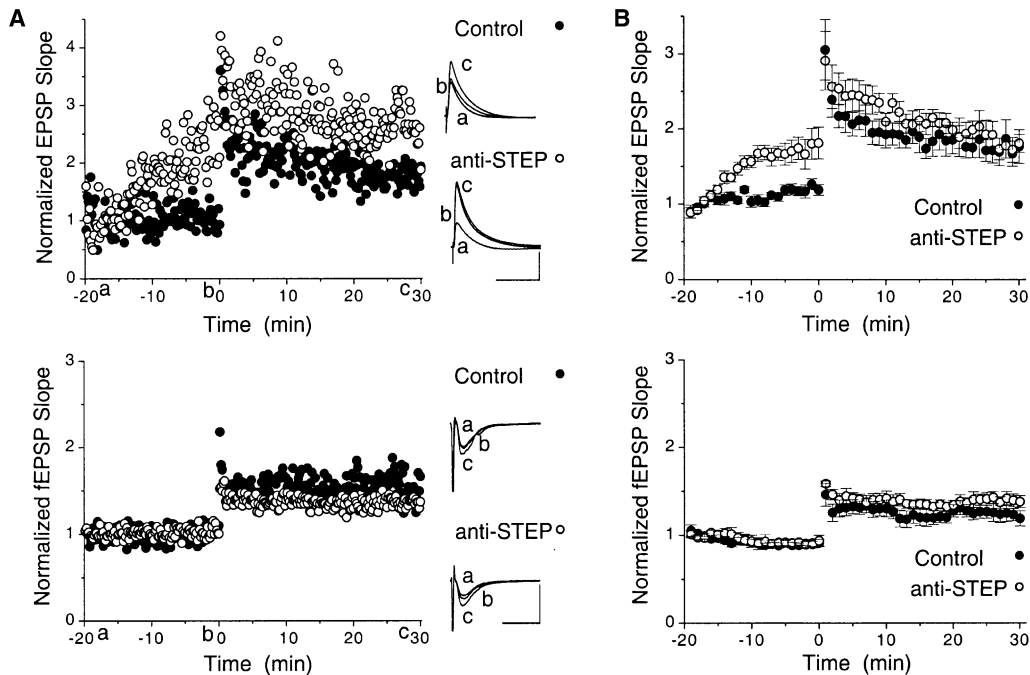


Figure 7. Inhibiting Endogenous STEP Enhances Synaptic Transmission and Occludes LTP at Schaffer Collateral CA1 Synapses

(A) Scatter plots of EPSP slope (upper graph) and simultaneously recorded fEPSP slope (lower graph) from individual experiments with (○) or without (●) anti-STEP in the whole-cell recording solution are shown. Each trace to the right of the plots is the average of six consecutive EPSPs or fEPSPs recorded at the times indicated.

(B) The top graph is a plot of average EPSP slope versus time for experiments with (○, $n = 9$) or without (●, $n = 8$) anti-STEP included in the whole-cell recording solution. The bottom graph shows averaged slope of field EPSPs (fEPSPs) measured during experiments when whole-cell recordings were done with (○) and without anti-STEP (●).

phorylation/dephosphorylation (Figures 2,3,5, and 8 and Huang et al., 2001; Lu et al., 1998; O'Dell et al., 1991), we reason that STEP acts upstream of AMPARs. Initiation of the LTP signaling cascade by tetanic stimulation requires an acute increase in NMDAR function, such as that which may be brought about by suppressing Mg^{2+} inhibition (Herron et al., 1986) or by activating Src (Ali and Salter, 2001). Given that the enhancement of synaptic transmission by inhibiting STEP is prevented by blocking NMDARs or the Src-dependent upregulation of NMDARs, the most parsimonious explanation for our results is that in CA1 neurons, STEP tonically suppresses NMDAR function and this suppression must be overcome in order to induce LTP.

When the anti-STEP antibody or the dominant-inhibitor STEP mutant protein was administered into CA1 neurons, we found that EPSPs increased, even when the frequency of synaptic stimulation was low. We have previously shown that synaptic AMPAR responses are similarly potentiated by intracellularly administering exogenous Src, a Src-activating peptide (Lu et al., 1998), or the Src-activating kinase $CAK\beta/Pyk2$ (Huang et al., 2001). As with the presently reported effects of anti-STEP, the potentiation of AMPAR responses induced by Src kinase, or its activators, is prevented by blocking NMDARs or by strongly buffering intracellular Ca^{2+} . In contrast, strongly buffering Ca^{2+} does not prevent the enhancement of NMDAR currents by anti-STEP or by Src. Together these results imply that the potentiation of AMPAR responses is dependent upon an NMDAR-

mediated rise in $[Ca^{2+}]_i$. At first glance, these observations might appear contrary to the concept that NMDARs are said to be "blocked" at the resting membrane potential by Mg^{2+} . However, even with physiological concentrations of extracellular Mg^{2+} , the current through NMDARs is not completely blocked at membrane potentials near rest (MacDonald et al., 1982), although this current is dramatically suppressed in comparison with depolarized potentials. Furthermore, recent work demonstrates that synaptically activating NMDARs in CA1 neurons at the resting membrane potential produces Ca^{2+} influx into dendritic spines (Kovalchuk et al., 2000). Our present findings indicate that inhibiting STEP enhances pharmacologically isolated NMDAR EPSCs recorded from neurons held near resting potential in the presence of extracellular Mg^{2+} (Figure 4). Therefore, the rise in $[Ca^{2+}]_i$ produced within dendritic spines by EPSPs at the resting potential would be increased by the enhancement of NMDAR function produced by inhibiting STEP and may thus bypass the requirement for tetanic stimulation to trigger LTP induction. It is unlikely that inhibiting STEP causes suppression of Mg^{2+} inhibition because the enhancement of NMDAR EPSCs by inhibiting STEP did not alter the NMDAR current-voltage relationship. It is possible, however, that inhibiting STEP may additionally act by facilitating processes downstream of, or in parallel to, Ca^{2+} entry through NMDARs that contribute to enhancement of AMPAR responses.

Our present findings indicate that the range over which NMDAR currents are regulated by activating or

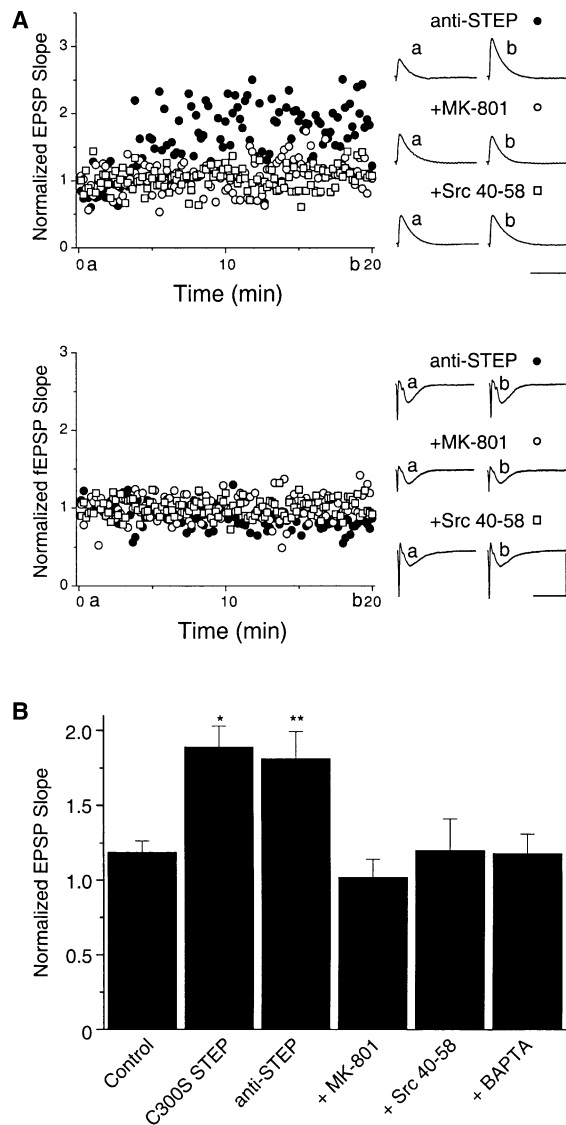


Figure 8. Enhancement of EPSPs by STEP Inhibition Requires NMDARs, Src Activity, and Ca^{2+}

(A) Scatter plots of EPSP slope (upper graph) and simultaneously recorded fEPSP slope (lower graph) from individual experiments with anti-STEP in the recording solution in the absence (●) or presence (○) of MK801 (1 μ M) and in the presence of Src 40-58 (0.03 mg/ml; □) are shown. Each trace on the right is the average of six consecutive EPSPs/fEPSPs recorded at the times indicated. Note that the data plotted for anti-STEP alone are from a different cell than that used for Figure 6A.

(B) A summary bar graph displaying the mean normalized EPSP slope 20 min after breakthrough in neurons recorded with control ICS (control, $n = 8$), C300S STEP containing ICS (C300S STEP, $n = 4$), anti-STEP containing ICS (anti-STEP, $n = 9$), anti-STEP containing ICS with MK801 in the bathing solution (+MK801, $n = 4$), ICS supplemented with both anti-STEP and Src 40-58 (+Src 40-58, $n = 4$), or ICS supplemented with both anti-STEP and 10 mM BAPTA (+BAPTA, $n = 7$) is shown. (* $p < 0.05$, ** $p < 0.01$, t test versus ICS.)

inhibiting STEP matches that produced by inhibiting or activating Src, respectively. Thus, STEP appears to account for the PTP activity opposing Src. Other PTPs, namely PTP1D (Husi et al., 2000; Lin et al., 1999) and

PTPMEG (Hironaka et al., 2000), have been reported to co-precipitate with NMDARs, but the effects of these PTPs on NMDAR function are unknown. PTPMEG is reported to promote Fyn-dependent phosphorylation of the GluRepsilon1 (NR2A) subunit (Hironaka et al., 2000), thus it seems unlikely that this phosphatase depresses NMDAR function since Fyn has been demonstrated to upregulate currents mediated by recombinant NMDARs expressed in HEK293 cells (Kohr and Seeburg, 1996). For PTP1D, or other PTPs that might also associate with NMDARs, while it is conceivable that these might participate in downregulating NMDAR channel activity, our results indicate that such effects would be dependent upon STEP in CA1 and dorsal horn neurons. Alternative, or additional, functional roles for these PTPs might be in processes other than modulating NMDAR channel activity, such as in regulating NMDAR targeting or trafficking (Dunah and Standaert, 2001; Vissel et al., 2001). Whether, in other cell types, there are PTP(s) that are able to subserve the same function as STEP does in CA1 and dorsal horn neurons remains to be determined.

Regulation of NMDAR function is critical to the development, maintenance, and plasticity of synaptic contacts (Dingledine et al., 1999; McBain and Mayer, 1994). Therefore, identification of specific proteins and processes that modulate NMDA channel function may be crucial in understanding the mechanisms by which synaptic transmission is controlled. Our results indicate that NMDAR-associated STEP tonically depresses channel activity to regulate synaptic efficacy. Because STEP is expressed in various regions of the nervous system (Boulanger et al., 1995) and tyrosine phosphorylation has been implicated in synaptic plasticity in a number of CNS areas (Boxall et al., 1996; Rosenblum et al., 1996, 1997; Rostas et al., 1996), we expect that this role of STEP may be a common mechanism for regulating excitatory synaptic transmission in many regions of the CNS.

Experimental Procedures

Coimmunoprecipitation of STEP and NMDARs

Striatal and hippocampal homogenates were prepared from male adult rats. The tissue was homogenized in 10 vol of ice-cold HEPES-buffered sucrose (0.32 M sucrose, 4 mM HEPES, 1 mM sodium orthovanadate, 1 mM phenylmethylsulfonyl fluoride, 2 μ g/ml pepstatin A, 2 μ g/ml leupeptin, and 2 μ g/ml aprotinin, pH 7.4) and centrifuged at $800 \times g$ for 10 min at $4^\circ C$ to remove nonhomogenized material (Paul et al., 2000). Crude synaptosomes were prepared from the striatum of male adult rats according to methods used for whole forebrain as described elsewhere (Huang et al., 2001). Fetal spinal cord membranes were prepared by methods adapted from Sheng et al. (1992). The spinal cords were homogenized in ice-cold Tris buffer (50 mM tris-HCl, 1 mM sodium orthovanadate, 1 mM phenylmethylsulfonyl fluoride, 20 μ g/ml pepstatin A, 20 μ g/ml leupeptin, and 20 μ g/ml aprotinin, pH 7.4) and centrifuged at $270 \times g$ for 10 min at $4^\circ C$ to remove debris. Immunoprecipitation of membrane proteins under nondenaturing and denaturing conditions was performed as previously described (Yu et al., 1997). For nondenaturing conditions, fetal membrane proteins were solubilized in ice-cold 50 mM tris-HCl (pH 7.6) containing 150 mM NaCl, 1% igepal ca630, 0.5% deoxycholate, 0.1% SDS, 1 mM orthovanadate, and the protease inhibitors pepstatin A (20 μ g/ml), leupeptin (20 μ g/ml), aprotinin (20 μ g/ml), and phenylmethylsulfonyl fluoride (1 mM). For denaturing conditions, membrane proteins were boiled in 1% SDS followed by 5-fold dilution with 50 mM tris-HCl (pH 7.6) containing 190 mM NaCl, 1.25% Triton X-100, 1 mM sodium orthovanadate, 6 mM EDTA, and the protease inhibitors listed above. Solubilized proteins (300 μ g)

were centrifuged at $14,000 \times g$ to remove insoluble material and then incubated with anti-NR1 (5 μg), anti-STEP (1/500 dilution), anti-GluR2 (5 μg), or nonspecific IgG (5 μg) overnight at 4°C . Immune complexes were isolated by adding 50 μl of protein G-Sepharose beads and incubating for 1 hr at 4°C . Immunoprecipitates were washed five times with lysis buffer and resuspended in $2 \times$ Laemmli sample buffer and boiled for 5 min. The samples were then subjected to SDS-polyacrylamide gel electrophoresis (SDS-PAGE) (10% gel) and then transferred to nitrocellulose membranes which were probed with anti-NR1 (0.5 $\mu\text{g/ml}$), anti-STEP (1/1000), or anti-GluR2 (1 $\mu\text{g/ml}$).

Single-Channel Patch-Clamp Recordings from Cultured Neurons

Primary cultures of spinal dorsal horn were prepared from fetal Wistar rats (embryonic day 17–18) (Salter and Hicks, 1994). Briefly, the spinal cord was removed from each fetus, and the dorsal half of the cord was dissected. Dorsal horn cells were isolated and plated in MEM supplemented with 10% FBS, 10% heat-inactivated horse serum, and 1 U/ml insulin. Cultures were used 10–24 days after plating. Media and sera were from Life Technologies (Burlington, Ontario, Canada). Single-channel recordings and analyses from inside-out patches are described by Yu et al., 1997. Cultures were bathed in extracellular solution containing (in mM): 80 Na_2SO_4 , 10 Cs_2SO_4 , 25 HEPES, 1.3 CaCl_2 , 33 glucose, 0.003 glycine, and 0.001 tetrodotoxin, pH 7.35 (310–325 mOsm). NMDA channel activity was evoked by including 0.01 mM NMDA in the extracellular solution contained within patch pipettes. Once a patch was pulled from the cell, the tip of the recording pipette was removed to a small reservoir where the intracellular aspect of the patch was perfused with intracellular solution composed of (in mM): 140 CsCl, 10 HEPES, 1 CaCl_2 , 10 BAPTA, 2 MgCl_2 , 4 $\text{K}_2\text{-ATP}$, pH 7.25 (310–325 mOsm) supplemented where indicated with recombinant STEP₄₆-GST (5 $\mu\text{g/ml}$). Patches were held at +70 mV and current records were stored on tape. For analysis, recordings were replayed, filtered at 2 kHz, and sampled at 20 kHz onto a computer using the fetchex program of the pClamp7 suite (Axon Instruments). Channel openings and closings were determined using the 50% crossing threshold method. Channel activity during a control period 4–7 min immediately preceding enzyme application was compared with activity during a similar period beginning 1–2 min after the start of the application.

Miniature EPSC Recordings

Methods for whole-cell recordings are described by Wang et al. (1996). Cultures were bathed in extracellular solution containing (in mM): 140 NaCl, 5.4 KCl, 25 HEPES, 1.3 CaCl_2 , 33 glucose, 0.001 glycine, 0.001 tetrodotoxin, 0.01 bicuculline, 0.01 strychnine, pH 7.35 (310–320 mOsm). The extracellular solution was supplemented where indicated with 50 mM PP2 or PP3 (Calbiochem, La Jolla, CA) or 0.05 mM AP5 (Sigma). Patch electrodes (4–7 M Ω) were filled with intracellular solution containing (in mM): 140 CsCl, 10 HEPES, 10 BAPTA, 2 Mg-ATP , pH 7.25 (300–310 mOsm). The intracellular solution was supplemented as required with STEP₄₆-GST (5 $\mu\text{g/ml}$), mutant C300S STEP₄₆-GST (5 $\mu\text{g/ml}$), anti-STEP antibody (23E5) (1:200 dilution), or nonspecific immunoglobulin G (IgG) antibody (1:200 dilution) and the osmolarity was readjusted accordingly. Membrane potential was held constant at -60 mV and whole-cell currents were recorded using an Axopatch 200B amplifier (Axon Instruments, Foster City, CA). Miniature EPSCs were recorded immediately upon formation of the whole-cell patch configuration and continuously monitored for 20–30 min thereafter. Miniature EPSCs were filtered at 2 kHz and acquired online with a personal computer using Strathclyde software (courtesy of J. Dempster) with the detection level set to approximately three times higher than the baseline noise. False events and traces with more than 1 event per 200 ms recording period were eliminated by subsequent inspection of the raw data, and averages were created using a minimum of 30 traces aligned by their rising edges. All recordings from cultured neurons were performed at room temperature (22°C – 24°C).

Phosphatase Activity Assay

PTP activity was measured in vitro using paranitrophenyl phosphate (pNPP) as substrate. PTP assays were performed in imidazole buffer

with 1% Triton X-100, pH 6.2, with 1.9 mM pNPP for 30 min at 30°C , and the reactions were terminated by adding 900 μl of 0.2N NaOH. The production of paranitrophenolate ion was expressed as a concentration using a molar extinction coefficient of $1.78 \times 10^4 \text{ M}^{-1} \text{ cm}^{-1}$ at 410 nm. The activities of recombinant STEP₄₆-GST or truncated T cell phosphatase (Calbiochem, La Jolla, CA) were measured with or without a 4-fold excess of anti-STEP antibody or with a nonspecific IgG (Figure 3A2 inset). The K_{cat} for STEP was decreased from 213 ± 13 mole/mole/min (mean \pm SEM, $n = 6$) to 30 ± 1.7 mole/mole/min ($n = 3$; $p < 0.01$, t test) with anti-STEP. In contrast, the activity of truncated T cell phosphatase was not affected by the anti-STEP antibody: K_{cat} – control, 3360 ± 220 mole/mole/min, $n = 3$; with anti-STEP, 3433 ± 217 , $n = 3$ ($p > 0.1$). In other experiments, we tested anti-STEP on the activity of PTP-1B (Calbiochem, La Jolla, CA). The K_{cat} for PTP1B was unaffected by the antibody: 1818 ± 62 mole/mole/min ($n = 4$) without versus 1750 ± 29 mole/mole/min with anti-STEP ($n = 3$).

Hippocampal Slice Recordings

Acute hippocampal slices were prepared from 4- to 6-week-old male Sprague Dawley rats and were placed in a holding chamber for at least 1 hr prior to recording (Lu et al., 1998). A single slice was transferred to a recording chamber and superfused with artificial cerebral spinal fluid (ACSF, 2 ml/min) composed of (in mM): 124 NaCl, 3 KCl, 1.25 NaH_2PO_4 , 2 MgCl_2 , 2 CaCl_2 , 26 NaHCO_3 , 10 D-glucose , 0.005 bicuculline methiodide, saturated with 95% O_2 –5% CO_2 at $30^\circ\text{C} \pm 2^\circ\text{C}$ (pH 7.35; 310–320 mOsm). Synaptic responses were evoked with bipolar tungsten electrodes placed approximately 50 μm from the cell body layer in CA1. Test stimuli were delivered at 0.1 Hz with the stimulus intensity set to 25% of that which produced maximum synaptic responses. Tetanic stimulation consisted of two trains of 100 Hz stimuli lasting 500 ms, with an intertrain interval of 10 s. In controls, this stimulation caused LTP that was at a stable level by 30 min after tetanus and which persisted for greater than 1 hr. For clarity of presentation, we show records from only the first 30 min after tetanic stimulation. EPSP slope was calculated as the slope of the rising phase 10%–65% of the peak response. Field potential recordings were made with glass micropipettes filled with ACSF placed in the stratum radiatum 60–80 μm from the cell body layer and 100–150 μm from the site of whole-cell recording. Field EPSP slope was calculated as the slope of the rising phase between 10% and 60% of the peak response. For current-clamp experiments, the patch pipette (4–6 M Ω) solution contained 132.5 mM K-glucuronate, 17.5 mM KCl, 10 mM HEPES, 0.2 mM EGTA, 2 mM Mg-ATP , 0.3 mM GTP, and 5 mM QX 314 (pH 7.25, 290 mOsm); EGTA was replaced with BAPTA (10 mM) where indicated. For voltage-clamp experiments, the intracellular solution contained: 132 mM Cs-glucuronate, 17 mM CsCl, 10 mM HEPES, 10 mM BAPTA, 2 mM Mg-ATP , 0.3 mM GTP, and 5 mM QX 314 (pH 7.25, 290 mOsm). The intracellular solutions were supplemented as required with recombinant STEP, anti-STEP antibody, IgG, C300S STEP, and Src 40-58 that were stored as single use stock solutions prepared just before use. Tetanic stimulation was delivered after 20 min of whole-cell recording. EPSP and fEPSP slopes were normalized to the respective average level during the first 5 min of whole-cell recording. Patch recordings were done using the “blind” patch method (Blanton et al., 1989). For recording NMDAR-mediated synaptic responses, ACSF was supplemented with DNQX (5 μM) and neurons were held at -60 mV. NMDAR-mediated EPSC peak amplitudes were normalized to the first 2 min of whole-cell recording. Current-voltage relationships for NMDA EPSCs were performed at the end of each recording and EPSC amplitude at each membrane potential was normalized on a cell-by-cell basis to that of the EPSC obtained at a holding potential of +40 mV. Raw data were amplified using an Axopatch 1-D, sampled at 10 kHz, and analyzed with Pclamp software (Axon Instruments, Foster City, CA). Series resistance ranged from 10 to 30 M Ω and cells were discarded if the resistance changed by more than 15%.

Acknowledgments

We thank Lu-Yang Wang, Leonard Kaczmarek, and John MacDonald for critical comments on the manuscript, and Janice Hicks for technical support. Supported by the Canadian Institutes of Health

Research (CIHR) (to M.W.S.), the National Institutes of Mental Health USA (to P.J.L.), and the Nicole Fealdman Memorial Fund (to M.W.S.). M.W.S. is a CIHR Investigator, K.A.P. is a CIHR Student, L.V.K. is a CIHR MD/PhD Student, G.M.P. is a CIHR Fellow, and R.A. was a Rick Hansen Foundation Fellow.

Received: October 22, 2001

Revised: January 10, 2002

References

- Ali, D.W., and Salter, M.W. (2001). NMDA receptor regulation by Src kinase signalling in excitatory synaptic transmission and plasticity. *Curr. Opin. Neurobiol.* **11**, 336–342.
- Arregui, C.O., Balsamo, J., and Lilién, J. (2000). Regulation of signaling by protein-tyrosine phosphatases: potential roles in the nervous system. *Neurochem. Res.* **25**, 95–105.
- Blanton, M.G., Lo Turco, J.J., and Kriegstein, A.R. (1989). Whole cell recording from neurons in slices of reptilian and mammalian cerebral cortex. *J. Neurosci. Methods* **30**, 203–210.
- Boulanger, L.M., Lombroso, P.J., Raghunathan, A., During, M.J., Wahle, P., and Naegele, J.R. (1995). Cellular and molecular characterization of a brain-enriched protein tyrosine phosphatase. *J. Neurosci.* **15**, 1532–1544.
- Boxall, A.R., Lancaster, B., and Garthwaite, J. (1996). Tyrosine kinase is required for long-term depression in the cerebellum. *Neuron* **16**, 805–813.
- Dingledine, R., Borges, K., Bowie, D., and Traynelis, S.F. (1999). The glutamate receptor ion channels. *Pharmacol. Rev.* **51**, 7–61.
- Dunah, A.W., and Standaert, D.G. (2001). Dopamine D1 receptor-dependent trafficking of striatal NMDA glutamate receptors to the postsynaptic membrane. *J. Neurosci.* **21**, 5546–5558.
- Edmonds, B., Gibb, A.J., and Colquhoun, D. (1995). Mechanisms of activation of glutamate receptors and the time course of excitatory synaptic currents. *Annu. Rev. Physiol.* **57**, 495–519.
- Hanke, J.H., Gardner, J.P., Dow, R.L., Changelian, P.S., Brissette, W.H., Weringer, E.J., Pollok, B.A., and Connelly, P.A. (1996). Discovery of a novel, potent, and Src family-selective tyrosine kinase inhibitor. Study of Lck- and FynT-dependent T cell activation. *J. Biol. Chem.* **271**, 695–701.
- Herron, C.E., Lester, R.A., Coan, E.J., and Collingridge, G.L. (1986). Frequency-dependent involvement of NMDA receptors in the hippocampus: a novel synaptic mechanism. *Nature* **322**, 265–268.
- Hironaka, K., Umemori, H., Tezuka, T., Mishina, M., and Yamamoto, T. (2000). The protein-tyrosine phosphatase PTPMEG interacts with glutamate receptor delta 2 and epsilon subunits. *J. Biol. Chem.* **275**, 16167–16173.
- Hollmann, M., and Heinemann, S. (1994). Cloned glutamate receptors. *Annu. Rev. Neurosci.* **17**, 31–108.
- Huang, Y., Lu, W., Ali, D.W., Pelkey, K.A., Pitcher, G.M., Lu, Y.M., Aoto, H., Roder, J.C., Sasaki, T., Salter, M.W., and MacDonald, J.F. (2001). $CAK\beta$ /Pyk2 kinase is a signaling link for induction of long-term potentiation in CA1 hippocampus. *Neuron* **29**, 485–496.
- Husi, H., Ward, M.A., Choudhary, J.S., Blackstock, W.P., and Grant, S.G. (2000). Proteomic analysis of NMDA receptor-adhesion protein signaling complexes. *Nat. Neurosci.* **3**, 661–669.
- Kohr, G. and Seeburg, P.H. (1996). Subtype-specific regulation of recombinant NMDA receptor-channels by protein tyrosine kinases of the src family. *J. Physiol. (Lond.)* **492**, 445–452.
- Kovalchuk, Y., Eilers, J., Lisman, J., and Konnerth, A. (2000). NMDA receptor-mediated subthreshold Ca^{2+} signals in spines of hippocampal neurons. *J. Neurosci.* **20**, 1791–1799.
- Lin, S.Y., Wu, K., Len, G.W., Xu, J.L., Levine, E.S., Suen, P.C., Mount, H.T., and Black, I.B. (1999). Brain-derived neurotrophic factor enhances association of protein tyrosine phosphatase PTP1D with the NMDA receptor subunit NR2B in the cortical postsynaptic density. *Brain Res. Mol. Brain Res.* **70**, 18–25.
- Lombroso, P.J., Murdoch, G., and Lerner, M. (1991). Molecular characterization of a protein-tyrosine-phosphatase enriched in striatum. *Proc. Natl. Acad. Sci. USA* **88**, 7242–7246.
- Lombroso, P.J., Naegele, J.R., Sharma, E., and Lerner, M. (1993). A protein tyrosine phosphatase expressed within dopaminergic neurons of the basal ganglia and related structures. *J. Neurosci.* **13**, 3064–3074.
- Lu, Y.M., Roder, J.C., Davidow, J., and Salter, M.W. (1998). Src activation in the induction of long-term potentiation in CA1 hippocampal neurons. *Science* **279**, 1363–1368.
- Lu, W.Y., Xiong, Z.G., Lei, S., Orser, B.A., Dudek, E., Browning, M.D., and MacDonald, J.F. (1999). G-protein-coupled receptors act via protein kinase C and Src to regulate NMDA receptors. *Nat. Neurosci.* **2**, 331–338.
- MacDonald, J.F., Porietis, A.V., and Wojtowicz, J.M. (1982). L-Aspartic acid induces a region of negative slope conductance in the current-voltage relationship of cultured spinal cord neurons. *Brain Res.* **237**, 248–253.
- Malenka, R.C., and Nicoll, R.A. (1999). Long-term potentiation—a decade of progress? *Science* **285**, 1870–1874.
- Malinow, R., Mainen, Z.F., and Hayashi, Y. (2000). LTP mechanisms: from silence to four-lane traffic. *Curr. Opin. Neurobiol.* **10**, 352–357.
- McBain, C.J., and Mayer, M.L. (1994). N-Methyl-D-aspartic acid receptor structure and function. *Physiol. Rev.* **74**, 723–760.
- Naegele, J.R., and Lombroso, P.J. (1994). Protein tyrosine phosphatases in the nervous system. *Crit. Rev. Neurobiol.* **9**, 105–114.
- O'Dell, T.J., Kandel, E.R., and Grant, S.G. (1991). Long-term potentiation in the hippocampus is blocked by tyrosine kinase inhibitors. *Nature* **353**, 558–560.
- Oyama, T., Goto, S., Nishi, T., Sato, K., Yamada, K., Yoshikawa, M., and Ushio, Y. (1995). Immunocytochemical localization of the striatal enriched protein tyrosine phosphatase in the rat striatum: a light and electron microscopic study with a complementary DNA-generated polyclonal antibody. *Neuroscience* **69**, 869–880.
- Paul, S., Snyder, G.L., Yokokura, H., Picciotto, M.R., Nairn, A.C., and Lombroso, P.J. (2000). The Dopamine/D1 receptor mediates the phosphorylation and inactivation of the protein tyrosine phosphatase STEP via a PKA-dependent pathway. *J. Neurosci.* **20**, 5630–5638.
- Rosenblum, K., Dudai, Y., and Richter-Levin, G. (1996). Long-term potentiation increases tyrosine phosphorylation of the N-methyl-D-aspartate receptor subunit 2B in rat dentate gyrus in vivo. *Proc. Natl. Acad. Sci. USA* **93**, 10457–10460.
- Rosenblum, K., Berman, D.E., Hazvi, S., Lamprecht, R., and Dudai, Y. (1997). NMDA receptor and the tyrosine phosphorylation of its 2B subunit in taste learning in the rat insular cortex. *J. Neurosci.* **17**, 5129–5135.
- Rostas, J.A., Brent, V.A., Voss, K., Errington, M.L., Bliss, T.V., and Gurd, J.W. (1996). Enhanced tyrosine phosphorylation of the 2B subunit of the N-methyl-D-aspartate receptor in long-term potentiation. *Proc. Natl. Acad. Sci. USA* **93**, 10452–10456.
- Salter, M.W., and Hicks, J.L. (1994). ATP-evoked increases intracellular calcium in cultured neurones and glia from the dorsal spinal cord. *J. Neurosci.* **14**, 1563–1575.
- Sheng, M., Tsaur, M.-L., Jan, Y.N., and Jan, L.Y. (1992). Subcellular segregation of two A-type K^+ channel proteins in rat central neurons. *Neuron* **9**, 271–284.
- Soderling, T.R., and Derkach, V.A. (2000). Postsynaptic protein phosphorylation and LTP. *Trends Neurosci.* **23**, 75–80.
- Stoker, A.W. (2001). Receptor tyrosine phosphatases in axon growth and guidance. *Curr. Opin. Neurobiol.* **11**, 95–102.
- Stoker, A., and Dutta, R. (1998). Protein tyrosine phosphatases and neural development. *Bioessays* **20**, 463–472.
- Tonks, N.K., and Neel, B.G. (2001). Combinatorial control of the specificity of protein tyrosine phosphatases. *Curr. Opin. Cell Biol.* **13**, 182–195.
- Vissel, B., Krupp, J.J., Heinemann, S.F., and Westbrook, G.L. (2001).

A use-dependent tyrosine dephosphorylation of NMDA receptors is independent of ion flux. *Nat. Neurosci.* 4, 587–596.

Wang, Y.T., and Salter, M.W. (1994). Regulation of NMDA receptors by tyrosine kinases and phosphatases. *Nature* 369, 233–235.

Wang, Y.T., Yu, X.M., and Salter, M.W. (1996). Ca²⁺-independent reduction of N-methyl-D-aspartate channel activity by protein tyrosine phosphatase. *Proc. Natl. Acad. Sci. USA* 93, 1721–1725.

Yu, X.M., Askalan, R., Keil, G.J., and Salter, M.W. (1997). NMDA channel regulation by channel-associated protein tyrosine kinase Src. *Science* 275, 674–678.